Journal of Membrane Science 349 (2010) 380–384

Contents lists available at ScienceDirect

Journal of Membrane Science

journal homepage: www.elsevier.com/locate/memsci

Inhibition of hydrogen transport through Pd and $Pd_{47}Cu_{53}$ membranes by H_2S at 350 °C

Casey P. O'Brien[a,b], Bret H. Howard[a,*], James B. Miller[a,b], Bryan D. Morreale[a], Andrew J. Gellman[a,b]

[a] National Energy Technology Laboratory, US Department of Energy, P.O. Box 10940, Pittsburgh, PA 15236, United States
[b] Department of Chemical Engineering, Carnegie Mellon University, Pittsburgh, PA 15213, United States

ARTICLE INFO

Article history:
Received 11 June 2009
Received in revised form 2 November 2009
Accepted 30 November 2009
Available online 4 December 2009

Keywords:
Palladium–copper membrane
Hydrogen sulfide
Palladium sulfide
Sulfur poisoning

ABSTRACT

In pure H_2 gas, hydrogen fluxes through pure Pd and $Pd_{47}Cu_{53}$ (mol%) foils at 350 °C are similar. In the presence of 1000 ppm H_2S in H_2, the hydrogen fluxes through both foils are substantially reduced, but with significantly different decay patterns. Six hours after the start of H_2S exposure, the Pd foil remained permeable to hydrogen, with the flux decreasing slowly over time. Analysis of the Pd foil by X-ray diffraction (XRD) and scanning electron microscopy (SEM) reveals that Pd reacts with H_2S to form a palladium sulfide corrosion product, Pd_4S, which is about 6.6 μm thick. These observations are consistent with the slow growth of a low-permeability, but catalytically active, sulfide corrosion layer on the Pd surface. In contrast, the hydrogen flux through the $Pd_{47}Cu_{53}$ foil is undetectable within 5 min of the start of H_2S exposure. XPS depth profiling of the $Pd_{47}Cu_{53}$ foil reveals that sulfur penetrates only ~3 nm into the $Pd_{47}Cu_{53}$ surface. Rapid formation of a Pd–Cu–S terminal layer, which is either inactive for hydrogen dissociation or impermeable to hydrogen atoms, is responsible for the deactivation of the $Pd_{47}Cu_{53}$ alloy membrane in H_2S at 350 °C.

1. Introduction

State-of-the-art gasification processes are being developed to reduce both foreign oil dependence and greenhouse gas emissions. Coal will be a primary fuel source for these processes and will produce a variety of secondary energy products including hydrogen, liquid fuels, and electricity with near-zero greenhouse gas emissions. Generating hydrogen from coal presents significant technical challenges, including the need to separate hydrogen from mixed gas streams composed primarily of H_2 and CO_2 with several minor constituents such as steam, CO, and H_2S.

Dense metal membranes are promising candidates for H_2/CO_2 separation due in part to their potential to produce high purity hydrogen and a high pressure CO_2-rich stream that is amenable to sequestration. Hydrogen permeates through metal membranes by means of a unique mechanism in which H_2 dissociatively adsorbs on the catalytically active surface of the metal, producing hydrogen atoms which diffuse through the interstices of the bulk metal lattice and recombine on the opposite surface. Only hydrogen atoms are able to diffuse through the bulk metal and an infinite selectivity for H_2 separation can be achieved. For sufficiently thick membranes with sufficiently high H_2 dissociation rates on the surface, hydrogen atom diffusion through the bulk limits the overall rate of hydrogen transport [1–10]. The performance of Pd membranes is distinguished from other pure metal membranes by the high H_2 dissociation activity of the Pd surface and the high hydrogen atom permeability of bulk Pd [11]. However, H_2S concentrations as low as parts-per-million (ppm) can severely corrode pure Pd membranes, compromising both the mechanical strength and high hydrogen permeability of the membrane [2,12–18].

To impart resistance to corrosion by H_2S, Pd has been alloyed with other metals [2,13,15,17,18]. Hydrogen transport through Pd–Cu alloys has received significant attention from both experimental and computational researchers [2–4,13,15–34]. The $Pd_{47}Cu_{53}$ (mol%) alloy has the highest hydrogen permeability at 350 °C among the Pd–Cu alloys [4,22,25,26], and is comparable in its hydrogen permeability to pure Pd at the same temperature. At higher temperatures (635 °C), hydrogen transport through $Pd_{47}Cu_{53}$ is not significantly inhibited by 1000 ppm H_2S [29]. At 350 °C, however, hydrogen transport through $Pd_{47}Cu_{53}$ is severely inhibited by H_2S [13,15,16,29]. In this report, we contrast the responses of Pd and $Pd_{47}Cu_{53}$ membranes to exposure to 1000 ppm H_2S at 350 °C. We analyze the compositions of the S-contaminated membranes by X-ray diffraction and X-ray photoelectron spectroscopy depth profiles to provide a framework for understanding the differences in their H_2S-induced performance degradation. This work shows that the pure Pd foil corrodes to form a thick (~μm) Pd_4S layer that retains some ability to dissociate and transport hydrogen. In contrast, the $Pd_{47}Cu_{53}$ alloy foil forms a very

* Corresponding author. Tel.: +1 412 386 5908; fax: +1 412 386 5920.
E-mail address: bret.howard@netl.doe.gov (B.H. Howard).

0376-7388/$ – see front matter © 2010 Published by Elsevier B.V.
doi:10.1016/j.memsci.2009.11.070

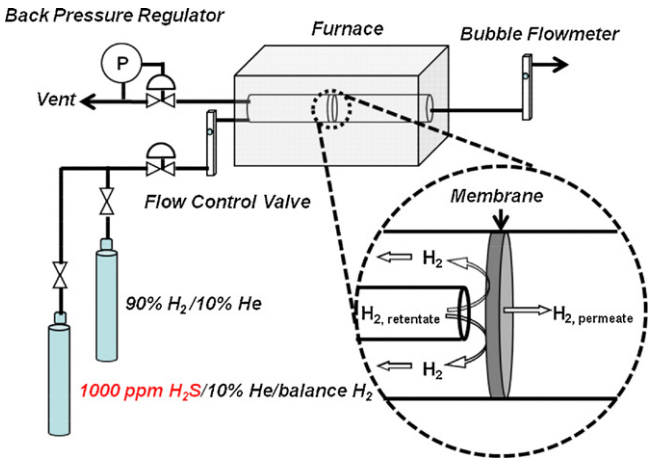

Fig. 1. Schematic of the membrane testing apparatus.

thin (~nm) Pd–Cu–S layer that is completely impermeable to hydrogen.

2. Experimental

Hydrogen transport measurements were performed using foil membranes of pure Pd and $Pd_{47}Cu_{53}$. Circular membrane foils were cut from 25 μm thick Pd (Alfa Aesar, 99.9% metals purity) and 25 μm thick $Pd_{47}Cu_{53}$ (ATI Wah Chang, 99.0% metals purity) foils. The membranes were washed with acetone and mounted into a Swagelok® VCR tube assembly. The effective membrane surface area was about 1.8 cm^2. Membranes were leak-tested by pressurizing the retentate (upstream) side of the membranes with 300 kPa of Ar and observing the pressure for 20 min. A leak-proof membrane was indicated by less than 1 kPa pressure drop on the upstream side. The leak-tested membrane tube assembly was then installed in the membrane testing apparatus which is shown schematically in Fig. 1.

Prior to making hydrogen permeation measurements, the membranes were heated to 350 °C in He (retentate, upstream) and Ar (permeate, downstream). Then the retentate sides of the membranes were exposed to a flowing mixture of 90% H_2/10% He (Butler Gas Products, Inc.) at 310 kPa, with the permeated H_2 collected

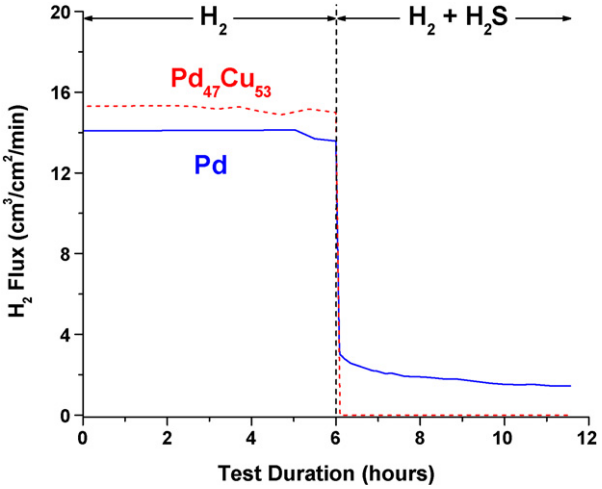

Fig. 2. Hydrogen flux through 25 μm Pd (blue solid line) and $Pd_{47}Cu_{53}$ (red dashed line) membranes versus test duration at 350 °C, total retentate pressure of 310 kPa and total permeate pressure of ~100 kPa (ambient pressure). A 90% H_2/10% He mixture was exposed to the membrane surface during the first portion of the test and then 1000 ppm H_2S/10% He/balance H_2 was fed to the membrane surface at 6 h.

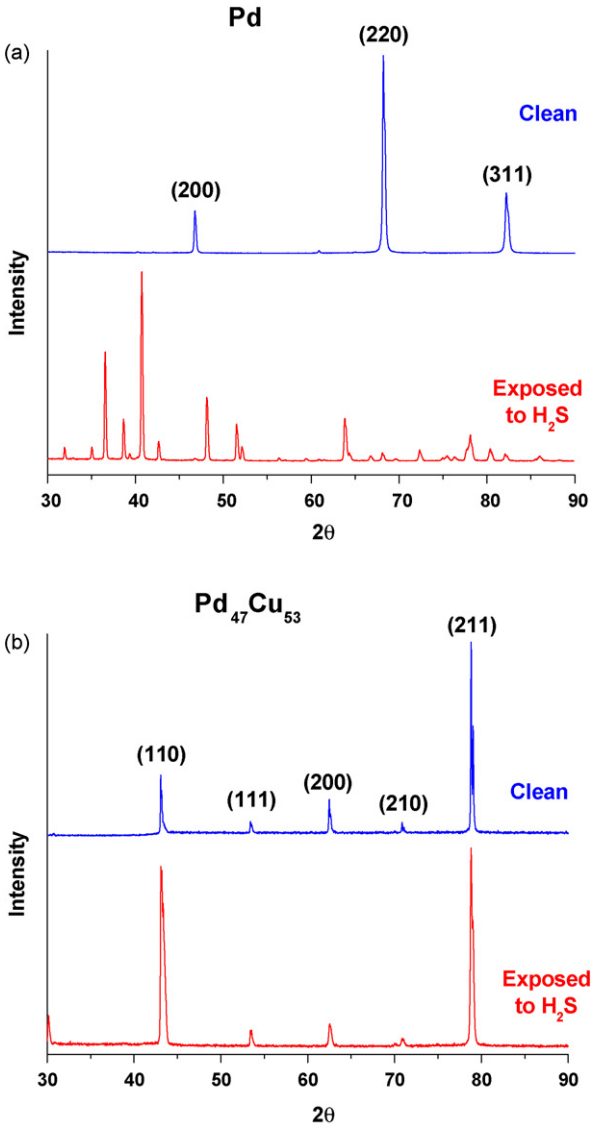

Fig. 3. X-ray diffraction patterns of (a) 25 μm Pd foil before (clean) and after exposure to 1000 ppm H_2S for 6 h (exposed to H_2S) and (b) 25 μm $Pd_{47}Cu_{53}$ foil before (clean) and after exposure to 1000 ppm H_2S for 6 h (exposed to H_2S).

at ambient pressure (~100 kPa). The temperature was measured using Omega type-K thermocouples positioned ~5 mm from the surface of each side of the membrane; the operating temperature was given by the average of the two temperatures. The H_2 flux through the membrane was measured using a bubble flowmeter (Alltech Digital Flowmeter Model 4074). A 1000 ppm H_2S/10% He/balance H_2 mixture (Butler Gas Products, Inc.) was introduced to the membrane surface following the 90% H_2/10% He mixture. The permeate gas composition was periodically analyzed by a gas chromatograph (Agilent Technologies Model 6890N) for its He content in order to confirm the absence of pinholes in the membrane. No He was detected in the permeate stream during the entire duration of the membrane tests, both before and during H_2S exposure. Following data collection, the membranes were cooled to room temperature in He and Ar and then dismounted for characterization.

X-ray diffraction (XRD) measurements of the foil surfaces were obtained using a PANalytical X'Pert Pro MPD powder diffractometer having a theta–theta configuration, a Cu X-ray source operated at 45 kV and 40 mA and an X'Celerator detector equipped with a monochromator. Patterns were recorded over a 2θ range of 30–90°

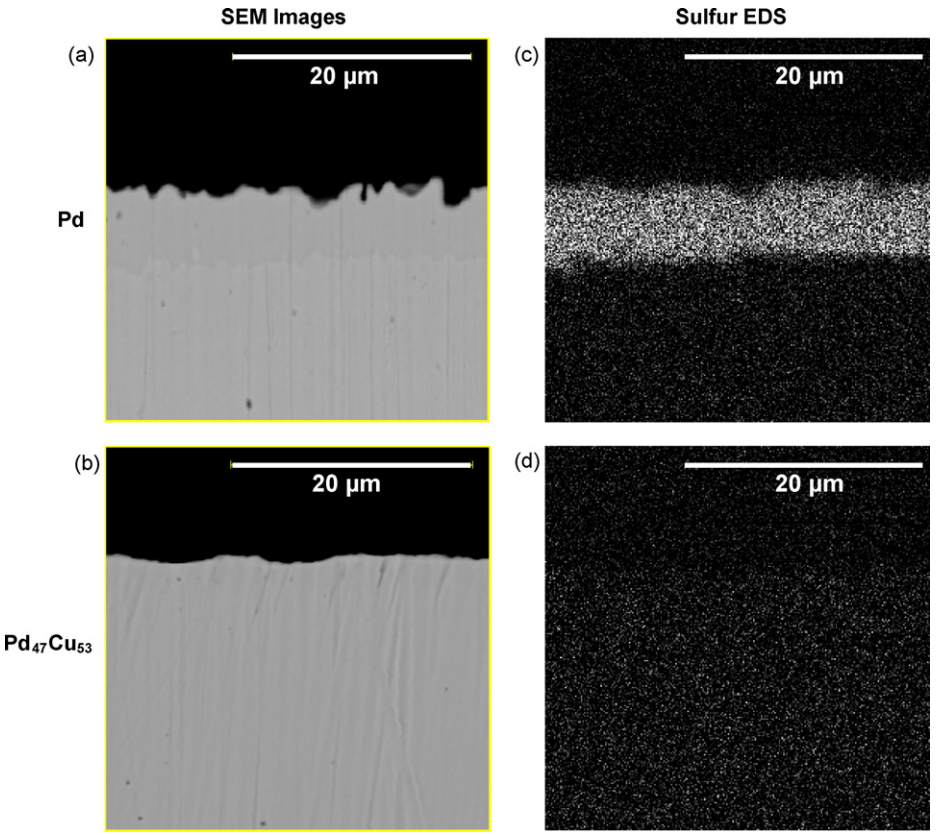

Fig. 4. Scanning electron micrographs of cross-sections of the (a) Pd and (b) $Pd_{47}Cu_{53}$ foils that were exposed to H_2S for 6 h. Sulfur X-ray mapping in the SEM images of the (c) Pd and (d) $Pd_{47}Cu_{53}$ cross-sections highlight the S-rich regions in white.

at a step size of 0.02°. Foil samples were mounted on zero background quartz slides for analysis. Sample foils were not perfectly flat resulting in a slight peak shape distortion; however this distortion did not affect data interpretation.

Scanning electron microscope (SEM) analysis of cross-sections of the foils was performed to determine the nature of the films grown on their surface during exposure to H_2S. Cross-sectioned pieces of the Pd and $Pd_{47}Cu_{53}$ foils were set in epoxy and then polished with Carbimet Paper (Buehler) up to 1200 grit. The polished cross-sections were then analyzed with an Aspex Personal SEM 2000 which was operated with a 20 keV electron beam. Sulfur X-ray maps of the cross-sections were used to quantify the thickness of the surface sulfide formed on the membrane foils.

X-ray photoelectron spectroscopy (XPS) measurements were used to determine the surface compositions of the foils and for depth profiling of the composition in the near-surface region. XPS measurements were performed on a PHI 5600ci instrument. The XPS instrument employed monochromatic aluminum K_α X-rays and the pass energy of the analyzer was 58.7 eV. Elemental surface concentrations were calculated from Cu $2p_{3/2}$, Pd $3d_{5/2}$, and S $2p_{3/2}$ peak areas and calibrated sensitivity factors. Depth profiles of elemental composition were acquired using Ar^+ as the sputtering gas and XPS analysis of surface composition. The differentially pumped ion gun was operated at 1.5×10^{-2} Pa and 25 mA, producing a sputtering rate of approximately10 nm/min based on calibration against the sputter rate of a 10 nm Pt film.

3. Results and discussion

Hydrogen fluxes through Pd and $Pd_{47}Cu_{53}$ membranes were measured, first in the absence of H_2S to establish a baseline, and then in the presence of 1000 ppm H_2S. Results of the membrane test are presented in Fig. 2. Baseline hydrogen fluxes through the two foils were ~14 $cm^3/cm^2/min$ for Pd and ~15 $cm^3/cm^2/min$ for $Pd_{47}Cu_{53}$. Assuming Sievert's Law is obeyed, the calculated H_2 permeabilities from the baseline H_2 fluxes were $\sim 1.3 \times 10^{-8}$ mol/m/s/$Pa^{1/2}$ for $Pd_{47}Cu_{53}$ and $\sim 1.2 \times 10^{-8}$ mol/m/s/$Pa^{1/2}$ for Pd; both are in good agreement with published permeability values [25,35]. The fact that these are so similar is expected; at 350 °C, the hydrogen permeability of body-centered-cubic $Pd_{47}Cu_{53}$ is known to be similar to that of the face-centered-cubic Pd [13,20,21,25]. Both membranes displayed significant decreases in hydrogen flux upon exposure to 1000 ppm H_2S. The hydrogen flux through the $Pd_{47}Cu_{53}$ foil was below the detection limit of the bubble flowmeter (<~0.06 $cm^3/cm^2/min$) within 5 min of H_2S exposure. In contrast, after an initially rapid decline, the hydrogen flux decay through the Pd foil slowed significantly. After 6 h of H_2S exposure, the hydrogen flux through the Pd membrane was still 10% of its baseline value.

To determine whether any thick metal-sulfide compounds (corrosion layers) formed as a result of H_2S exposure, the Pd and $Pd_{47}Cu_{53}$ foils were analyzed by X-ray diffraction (XRD) following membrane testing. Fig. 3(a) and (b) display the XRD patterns for the Pd and $Pd_{47}Cu_{53}$ foils, respectively, including diffraction patterns of the clean Pd and $Pd_{47}Cu_{53}$ foils for reference. As expected, the diffraction pattern of the clean Pd foil exhibits features that are assignable to the face-centered-cubic Pd structure. The XRD pattern of the Pd foil that was exposed to H_2S is dominated by features that can be assigned to crystalline palladium sulfide (Pd_4S), with only very small peaks from metallic Pd. These results illustrate that H_2S exposure causes the Pd membrane to form a specific palladium sulfide reaction product, Pd_4S; we have described the mechanism of this reaction in previous reports [12,13,18]. In contrast to the XRD results from the Pd foil, the XRD patterns of the clean $Pd_{47}Cu_{53}$ foil and the $Pd_{47}Cu_{53}$ foil after 6 h of H_2S exposure (Fig. 3(b)) are nearly identical and are both assignable to the

body-centered-cubic structure of $Pd_{47}Cu_{53}$. The diffraction peak intensities of the clean and H_2S-exposed $Pd_{47}Cu_{53}$ foils are not identical and vary from the intensities expected for an ideal body-centered-cubic $Pd_{47}Cu_{53}$ powdered sample. The peak intensities observed for the clean Pd foil also vary from the intensities expected for an ideal face-centered-cubic Pd powdered sample. These variations are probably due to the fact that non-ideal solid metal foil samples were analyzed. The discrepancies in peak intensity probably reflect a preferred orientation of the metal crystallites comprising the membrane foils.

Cross-sections of the Pd and $Pd_{47}Cu_{53}$ foils were imaged by SEM to determine the thickness of sulfur corrosion layers on the surface of the foils. The sulfur concentration was mapped over the SEM images by EDS. SEM analysis of the Pd and $Pd_{47}Cu_{53}$ foils after H_2S exposure are presented in Fig. 4(a) and (b), respectively; EDS mapping of sulfur concentration in the SEM images of the Pd and $Pd_{47}Cu_{53}$ foils are presented in Fig. 4(c) and (d), respectively. A noticeable difference in the roughness of the Pd and $Pd_{47}Cu_{53}$ foil surfaces exposed to H_2S is evident from the SEM images in Fig. 4; the surface of the Pd foil (Fig. 4(a)) is significantly rougher than that of the $Pd_{47}Cu_{53}$ foil (Fig. 4(b)). Sulfidation of the Pd foil surface to Pd_4S is probably responsible for the fact that the Pd foil surface is rougher than that of the $Pd_{47}Cu_{53}$ foil, which did not form any sulfur compounds that could be detected by XRD. EDS reveals a sulfur-rich layer on the surface of the Pd foil (Fig. 4(c)), which XRD identified as a Pd_4S film, that is $\sim 6.6 \pm 0.9$ μm thick (average of 75 different thickness measurements across the entire length of the Pd foil cross-section). In contrast to the sulfur film observed on the Pd foil, EDS (Fig. 4(d)) did not detect a significant amount of sulfur on the $Pd_{47}Cu_{53}$ foil after H_2S exposure. EDS analyzes X-rays from a relatively large volume within the sample, however, and thus it is not able to detect sulfur contamination in a very thin layer near the surface of the $Pd_{47}Cu_{53}$ membrane.

XPS depth profiles of the Pd and $Pd_{47}Cu_{53}$ foils were collected to detect sulfur contamination near the membrane surfaces that may be undetectable by XRD and EDS analysis. XPS composition depth profiles of the Pd and $Pd_{47}Cu_{53}$ foils after 6 h of H_2S exposure are presented in Fig. 5(a) and (b), respectively. The Pd foil (Fig. 5(a)) has a stoichiometry in the near-surface region (~200 nm) that is approximately constant at Pd:S ≈ 4:1, which is consistent with the presence of Pd_4S as indicated by the XRD results. In contrast, S appears only very near the top-surface of the $Pd_{47}Cu_{53}$ alloy membrane (Fig. 5(b)); its signal decayed to zero after Ar^+ sputtering only ~3 nm into the bulk of the $Pd_{47}Cu_{53}$ membrane.

Pd and $Pd_{47}Cu_{53}$ membranes clearly respond differently to H_2S exposure at 350 °C. We believe that the different responses in hydrogen flux to H_2S exposure exhibited by the two membranes are related to the evolution of their surface compositions during H_2S exposure. Furthermore, two different mechanisms may be responsible for the inhibition of hydrogen transport through the two membranes: poisoning of the catalytic dissociation of H_2 at the surface and reduced permeability of hydrogen through the bulk of the membrane.

The observation of non-zero flux through the Pd foil during H_2S exposure indicates that the membrane surface retained H_2 dissociation activity. The continuous slow decline of the hydrogen flux through the Pd membrane is indicative of an increasing resistance to hydrogen transport, which is consistent with hydrogen atom diffusion being retarded by a slowly thickening, dense, low-permeability Pd_4S corrosion layer on the surface. This mechanism has been suggested by Morreale et al. who estimated the hydrogen permeability of Pd_4S at 350 °C to be ~1/20th that of Pd by correlating Pd_4S growth kinetics to the decline in hydrogen flux through a Pd membrane during H_2S exposure [12,13]. The steep initial decline in hydrogen flux through the Pd membrane immediately following H_2S exposure may be due to a rapid initial corrosion rate that slows

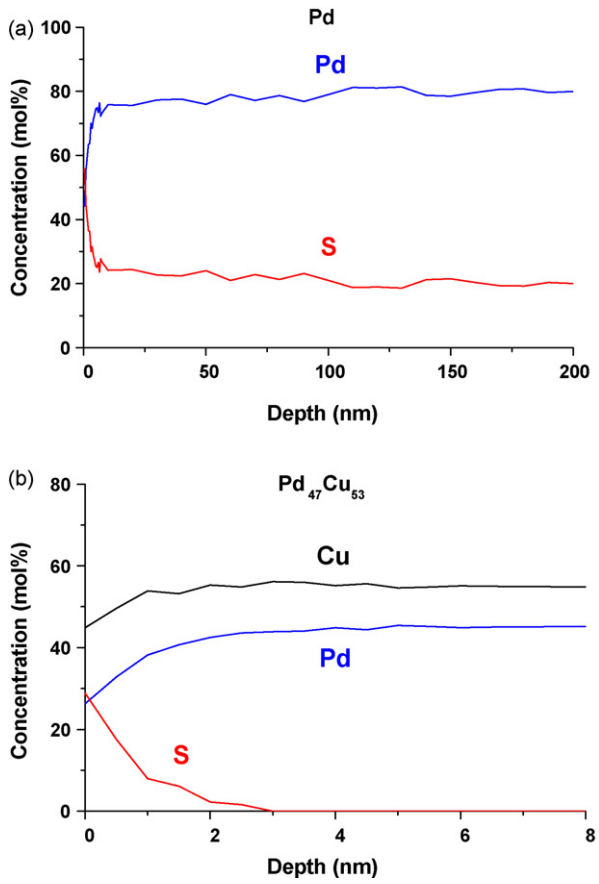

Fig. 5. X-ray photoelectron spectroscopy depth profiles of the (a) 25 μm Pd and (b) 25 μm $Pd_{47}Cu_{53}$ membranes exposed to 1000 ppm H_2S for 6 h. Elemental concentrations shown for Pd (blue), S (red), and Cu (black). The sputtering rate is ~10 nm/min as measured using a pure Pt film. (For interpretation of the references to color in this figure caption, the reader is referred to the web version of the article.)

as diffusion of Pd and/or S ions through the Pd_4S scale becomes slower. Another possible explanation for the rapid initial decline in hydrogen flux through the Pd membrane following H_2S exposure is that the catalytic activity of the Pd_4S surface may be significantly lower than that of Pd. As the thickness of the low-permeability Pd_4S film grows beyond a critical value, hydrogen atom diffusion through the bulk becomes rate limiting. A third explanation for the evolution of the hydrogen flux is that there may be a significant barrier to hydrogen atom transport across the Pd_4S/Pd interface that dominates transport initially but becomes insignificant as the Pd_4S thickness grows beyond a critical value.

The immediate decline in hydrogen flux through the $Pd_{47}Cu_{53}$ membrane at the start of H_2S exposure must be related to the properties of its thin Pd–Cu–S terminal layer. Neither XRD nor XPS depth profiling could identify this thin Pd–Cu–S terminal layer as a specific compound and, therefore, the mechanism of its formation is not clear. Presumably this layer is either inactive for hydrogen dissociation ("sulfur-poisoned") or it displays near-zero hydrogen atom permeability.

4. Conclusions

As expected, hydrogen fluxes through 25 μm Pd and $Pd_{47}Cu_{53}$ membranes at 350 °C were observed to be comparable in the absence of H_2S in the hydrogen feed. However, their interactions with H_2S, and the resulting effects of H_2S on hydrogen flux, were significantly different. Six hours of exposure of the Pd foil to 1000 ppm of H_2S at 350 °C resulted in the formation of a

thick (~6.6 μm) Pd_4S corrosion layer which, while exhibiting lower hydrogen atom permeability than pure Pd, retained its catalytic activity for H_2 dissociation. The slow flux decline observed for the Pd foil at longer H_2S exposure times is consistent with a Pd_4S corrosion layer that is continually growing. In contrast, the $Pd_{47}Cu_{53}$ membrane resisted bulk corrosion and sulfur penetrated less than ~3 nm into its surface. However, because the hydrogen flux through the alloy membrane was undetectable within 5 min of H_2S exposure, the thin Pd–Cu–S terminal layer that formed at the top-surface of the alloy must be inactive for hydrogen dissociation or impermeable to hydrogen atoms.

Acknowledgement

This technical effort was performed in support of the National Energy Technology Laboratory's on-going research in Computational and Basic Sciences under the RDS contract DE-AC26-04NT41817.

References

[1] I.B. Elkina, J.H. Meldon, Hydrogen transport in palladium membranes, Desalination 147 (2002) 445–448.
[2] M.V. Mundschau, X. Xie, C.R. Evenson, A.F. Sammells, Dense inorganic membranes for production of hydrogen from methane and coal with carbon dioxide sequestration, Catal. Today 118 (2006) 12–23.
[3] P.M. Thoen, F. Roa, J.D. Way, High flux palladium–copper composite membrane for hydrogen separations, Desalination 193 (2006) 224–229.
[4] L. Yuan, A. Goldbach, H. Xu, Segregation and H_2 transport rate control in body-centered cubic PdCu membranes, J. Phys. Chem. B 111 (2007) 10952–10958.
[5] T.B. Flanagan, D. Wang, K.L. Shanahan, Diffusion of H through Pd membranes: effects of non-ideality, J. Membr. Sci. 306 (2007) 66–74.
[6] H. Amandusson, L.-G. Ekedahl, H. Dannetun, Hydrogen permeation through surface modified Pd and PdAg membranes, J. Membr. Sci. 193 (2001) 35–47.
[7] S.-Y. Liu, Y.-H. Kao, Y. Oliver Su, T.-P. Perng, Analysis of hydrogen and deuterium absorption kinetics in Pd nanofilms, J. Alloys Compd. 311 (2000) 283–287.
[8] H. Li, H. Xu, W. Li, Study of *n* value and α/β palladium hydride phase transition within the ultra-thin palladium composite membrane, J. Membr. Sci. 324 (2008) 44–49.
[9] C.H.F. Peden, B.D. Kay, D.W. Goodman, Kinetics of hydrogen absorption by chemically modified Pd(110), Surf. Sci. 175 (1986) 215–225.
[10] F. Gallucci, F. Chiaravalloti, S. Tosti, E. Drioli, A. Basile, The effect of mixture gas on hydrogen permeation through a palladium membrane: experimental study and theoretical approach, Int. J. Hydrogen Energy 32 (2007) 1837–1845.
[11] K. Nobuhara, H. Kasai, W.A. Dino, H. Nakanishi, H_2 dissociative adsorption on Mg, Ti, Ni, Pd and La surfaces, Surf. Sci. 566–568 (2004) 703–707.
[12] B.D. Morreale, B.H. Howard, O. Iyoha, R.M. Enick, C. Ling, D.S. Sholl, Experimental and computational prediction of the hydrogen transport properties of Pd_4S, Ind. Eng. Chem. Res. 46 (2007) 6313–6319.
[13] B.D. Morreale, The Influence of H_2S on Palladium and Palladium–Copper Alloy Membranes, Chemical Engineering, vol. Doctor of Philosophy, University of Pittsburgh, 2006.
[14] D.J. Edlund, W.A. Pledger, Thermolysis of hydrogen sulfide in a metal-membrane reactor, J. Membr. Sci. 77 (1993) 255–264.
[15] D.L. McKinley, Metal alloy for hydrogen separation and purification, USA, 1967.
[16] P. Kamakoti, B.D. Morreale, M.V. Ciocco, B.H. Howard, R.P. Killmeyer, A.V. Cugini, D.S. Sholl, Prediction of hydrogen flux through sulfur-tolerant binary alloy membranes, Science 307 (2005) 569–573.
[17] O. Iyoha, R. Enick, R. Killmeyer, B. Howard, M. Ciocco, B. Morreale, H_2 production from simulated coal syngas containing H_2S in multi-tubular Pd and 80wt% Pd–20 wt% Cu membrane reactors at 1173 K, J. Membr. Sci. 306 (2007) 103–115.
[18] O. Iyoha, R. Enick, R. Killmeyer, B. Morreale, The influence of hydrogen sulfide-to-hydrogen partial pressure ratio on the sulfidization of Pd and 70 mol% Pd–Cu membranes, J. Membr. Sci. 305 (2007) 77–92.
[19] A. Kulprathipanja, G.O. Alptekin, J.L. Falconer, J.D. Way, Pd and Pd–Cu membranes: inhibition of H_2 permeation by H_2S, J. Membr. Sci. 254 (2005) 49–62.
[20] D.J. Edlund, Hydrogen-permeable metal membrane and method for producing the same, US Patent 6,152,995 (2000).
[21] B.H. Howard, R.P. Killmeyer, K.S. Rothenberger, A.V. Cugini, B.D. Morreale, R.M. Enick, F. Bustamante, Hydrogen permeance of palladium–copper alloy membranes over a wide range of temperatures and pressures, J. Membr. Sci. 241 (2004) 207–218.
[22] J.Y. Yang, C. Nishimura, M. Komaki, Effect of H_2S on hydrogen permeation of $Pd_{60}Cu_{40}$/V–15Ni composite membrane, J. Alloys Compd. (2007) 446–447.
[23] F. Roa, J.D. Way, R.L. McCormick, S.N. Paglieri, Preparation, Characterization of Pd–Cu composite membranes for hydrogen separation, Chem. Eng. J. 93 (2003) 11–22.
[24] S. Nam, Y. Seong, J.W. Lee, K. Lee, Preparation of highly stable palladium alloy composite membranes for hydrogen separation, Desalination 236 (2009) 51–55.
[25] D.L. McKinley, Method for hydrogen separation and purification, USA, 1969.
[26] F. Roa, M.J. Block, J.D. Way, The influence of alloy composition on the H_2 flux of composite Pd–Cu membranes, Desalination 147 (2002) 411–416.
[27] X. Zhang, W. Wang, J. Liu, S. Sheng, G. Xiong, W. Yang, Hydrogen transport through thin palladium–copper alloy composite membranes at low temperatures, Thin Solid Films 516 (2008) 1849–1856.
[28] J.Y. Yang, C. Nishimura, M. Komaki, Hydrogen permeation of $Pd_{60}Cu_{40}$ alloy covered V–15Ni composite membrane in mixed gases containing H_2S, J. Membr. Sci. 309 (2008) 246–250.
[29] B.D. Morreale, M.V. Ciocco, B.H. Howard, R.P. Killmeyer, A.V. Cugini, R.M. Enick, Effect of hydrogen-sulfide on the hydrogen permeance of palladium–copper alloys at elevated temperatures, J. Membr. Sci. 241 (2004) 219–224.
[30] L. Yuan, A. Goldbach, H. Xu, Real-time monitoring of metal deposition and segregation phenomena during preparation of PdCu membranes, J. Membr. Sci. 322 (2008) 39–45.
[31] S.M. Opalka, W. Huang, D. Wang, T.B. Flanagan, O.M. Lovvik, S.C. Emerson, Y. She, T.H. Vanderspurt, Hydrogen interactions with the PdCu ordered B2 alloy, J. Alloys Compd. 446–447 (2007).
[32] J.Y. Yang, C. Nishimura, M. Komaki, Effect of overlayer composition on hydrogen permeation of Pd–Cu alloy coated V–15Ni composite membrane, J. Membr. Sci. 282 (2006) 337–341.
[33] P. Kamakoti, D.S. Sholl, A comparison of hydrogen diffusivities in Pd and CuPd alloys using density functional theory, J. Membr. Sci. 225 (2003) 145–154.
[34] P. Kamakoti, D.S. Sholl, Ab initio based lattice gas modeling of interstitial hydrogen diffusion in CuPd alloys, Phys. Rev. B 71 (2005).
[35] R. Ngameni, C. Decaux, D. Solas, S. Grigoriev, P. Millet, Time and frequency domain analysis of hydrogen permeation across PdCu metallic membranes for hydrogen purification, Int. J. Hydrogen Energy (2009), doi:10.1016/j.ijhydene.2009.1008.1100.